



# Lattice-Boltzmann simulation of circular column coupled with square column in cross flow

Dongyan SHI<sup>1</sup>; Hongqun LI<sup>2</sup>; Zhikai WANG<sup>3</sup>; Han JIAO<sup>4</sup>

<sup>1</sup> Harbin Engineering University, China

<sup>2</sup> Harbin Engineering University, China

<sup>3</sup> Harbin Engineering University, China

<sup>4</sup> Harbin Engineering University, China

## ABSTRACT

Based on the single relaxation time lattice Boltzmann method, a numerical simulation model of fluid flow over two side-by-side columns is developed. One is a resting square column and the other is a circular cylinder which can rotate with a constant velocity. The calculation is carried out at a pitch ratios ( $S/D = 0.5$ , where  $S$  is the gap distance while  $D$  is the circular column diameter) at Reynolds number of 150. The effects of the curved boundary offset lattice links and the solid boundaries velocity is introduced into the model. Comparing the benchmark problem of fluid flow over a single column, the drag and lift forces ( $C_d$ ,  $C_l$ ) and the wake flow characteristics are studied to verify the model and investigate the interaction of the two columns. The results indicate that the interaction of the two columns has significant influence on dynamic characteristics of fluid flow over columns. The regular vortex shedding comes into irregular. The  $C_d$  and  $C_l$  increase under the effect of the interaction. Furthermore, with the rotating velocity is increased, the fluctuation of  $C_d$  and  $C_l$  becomes more serious.

Keywords: Side-by-side columns, Rotating, Lattice Boltzmann method  
I-INCE Classification of Subjects Number(s): 21.6

## 1. INTRODUCTION

It will produce complex flow phenomena when fluid flows through single or multiple-column structure, and form vortex field structures in different shapes at the end of the cylinder. The situation of vortex formation and shedding will cause periodic vibration of cylinder, vibration noise, and become radiation noise source in the flow field. The subject of experimental and numerical study on bluff-body flows is received more and more attention because of the complexity in flow phenomenon and the universal in real project field (1-3).

The disadvantage of experimental results is not easy to observe because conditions on experimental study are difficult to control. So, it is obvious that experimental investigation lags behind numerical simulation. In particular, numerical study about flow has been rapid development with the development of computational fluid dynamics (CFD), the presentation of a variety of numerical algorithms and the support of high-performance computing (4, 5). Lattice Boltzmann method (LBM) is a new method of CFD that has a fast-growing during the last twenty or thirty years, differing from conventional finite element, finite volume method (6). It comes from continuous Boltzmann equation, then evolves a single relaxation factor model around 1993 (7), and attracts people's attention quickly. In 1997, He et al. (8) investigated the flow patterns behind a circular cylinder using lattice Boltzmann method on a curvilinear coordinate system at low Reynolds numbers, and comparisons with other study results are satisfactory. The ability of method is demonstrated. In the flow situation, it is particularly important for the processing of fluid-solid boundary to reduce unnecessary numerical error. In 1993, Ziegler et al. (9) proposed a heuristic method for no-slip

---

<sup>1</sup> shidongyan@hrbeu.edu.cn

<sup>2</sup> lihongqun@hrbeu.edu.cn

<sup>3</sup> zhikai.wa@gmail.com

<sup>4</sup> Jiaohan199203@gmail.com

boundary condition. Its model contains the collisions operation among solid wall particles. In 2006, Niu X. et al. (10) presented a fluid-solid boundary method combining Immersed Boundary method and LBM that is based on the momentum exchange. Besides, in literature (11-14), fluid-solid boundary had been improved and optimized in varying degrees.

So far, Lattice Boltzmann on the fluid-solid boundary condition is quite mature, and serve as a basis for numerical simulation investigation of flow past a single cylinder is a great success. As a comparison, the phenomenon of flowing over multi - cylinder existing coupling effect is more complex , closer to practical engineering applications, but relatively fewer research (15, 16). Xu et al. (16) presented the flow characteristics between two vibrating side-by-side circular cylinders for Reynolds number of 200. Yang et al. (17) discussed the coupling effect among three circular cylinders in fluid filed using Boltzmann method, and, two of the cylinders are rigid and the other one is for the forced vibration at a frequency of 0.4. Vikram et al. (2) studied the coupling effect of flow over two square cylinders in tandem arrangement. The results showed the lift of upstream cylinder is higher than downstream. Patil et al. (18) extrapolated the distribution function across the cell boundaries based on finite volume formulation of the lattice Boltzmann equation. Agrawal et al. (15) used lattice Boltzmann method to simulated flow around a pair of side by side square cylinders. They studied the effects of the gap ratio  $\beta$  of 2.5, 2.0, 0.7 at  $Re=73$ .

On the basis of these studies, using the combination method of the LBM and finite difference method (14), the coupled model is established in viscous flow around two side by side cylinders that one is a circular cylinder and the other is a square cylinder. And a two-dimensional numerical simulation of flow over two cylinders with the gap ratio  $\beta = \Delta / D = 0.5$  is carried out. Interaction coupling between cylinders is investigated when the both are stationary. Another objective of this present work is to explore the effect of flow characteristics for the circular cylinder with rotating at a certain speed.

## 2. NUMERICAL METHOD

### 2.1 Lattice Boltzmann Method

The single relaxation time lattice Boltzmann method which originates from the continuous Boltzmann method can be written as

$$f_i(\mathbf{r} + \mathbf{e}_i \delta_t, t + \delta_t) - f_i(\mathbf{r}, t) = -\phi(f_i(\mathbf{r}, t) - f_i^{(0)}(\mathbf{r}, t)). \quad (1)$$

Where  $f_i(\mathbf{r}, t)$  is the number density of particles on the mesoscopic level and  $f_i^{(0)}(\mathbf{r}, t)$  stands for the equilibrium state that satisfies Max-well distribution,

$$f_i^{(0)}(\mathbf{r}, t) = w_i \rho (1 + 3(\mathbf{e}_i \cdot \mathbf{u}) + \frac{9}{2}(\mathbf{e}_i \cdot \mathbf{u})^2 - \frac{3}{2}\mathbf{u}^2). \quad (2)$$

$\mathbf{r}$  stands for the molecules position.  $\mathbf{e}_i$  is the lattice discrete particle velocity. For the D2Q9 model is adopted here,  $\mathbf{e}_i$  can be expressed as

$$\mathbf{e}_i = \begin{cases} (0, 0), i = 0 \\ (\cos(\frac{(i-1)}{2}\pi), \sin(\frac{(i-1)}{2}\pi)), i = 1, \dots, 4 \\ \sqrt{2}(\cos(\frac{(2i-9)}{4}\pi), \sin(\frac{(2i-9)}{2}\pi)), i = 5, \dots, 8 \end{cases}. \quad (3)$$

$\phi$  is the reciprocal value of relaxation parameter,  $\tau$ , which is related to the viscosity,  $\nu = \frac{\tau}{3} - \frac{1}{6}$ . The macroscopic variables like the fluid density  $\rho$  and velocity  $\mathbf{u}$  can be calculated,

$$\rho = \sum_{i=0}^8 f_i, \mathbf{u} = \sum_{i=0}^8 \mathbf{e}_i f_i / \rho. \quad (4)$$

In the works of Qian Y. et al. (7) and He X. et al. (19), it is found that the second-order Navier-Stokes equations can be recovered by Eq. (1) using the Cahn-Hilliard expression. the manuscript.

### 2.2 Boundary Condition

In this study, the boundary system is divided into two parts: one is the plane, straight and resting boundary, and the other is the curved and moving boundary. The former part is handled with Half-way

bounce back method, and the latter one is implemented combining the LBM and the finite difference method. The unknown distribution function ( $\tilde{f}_i$ ) after advection that comes from the solid nodes can be obtained using the following interpolation formulas:

$$\tilde{f}_i(\mathbf{r}_{fb}, t + \delta_t) = f_i^{eq}(\mathbf{x}_{fb}, t) - 6w_i \rho (\mathbf{e}_i \cdot \mathbf{u}_{mid}) . \tag{5}$$

In the above equation,  $\mathbf{r}_{fb}$  stands for the fluid node position that closed to the solid boundary. For the fluid density  $\rho$  and the velocity  $\mathbf{u}$  is known,  $f_i^{eq}(\mathbf{r}_{fb}, t)$  can be calculated directly. All the other parameters are kept consistent with those that defined above except the parameter  $\mathbf{u}_{mid}$ .  $\mathbf{u}_{mid}$  is the velocity of the virtual node that is located at the middle of  $\mathbf{r}_{fb}$  and  $\mathbf{r}_b$  as shown in Figure 1. Similarly to  $\mathbf{r}_{fb}$ ,  $\mathbf{r}_b$  is the solid node position that closed to the solid boundary.

After advection, the distribution functions  $f_i$  at  $\mathbf{r}_{fb}$  that come from the boundary direction is unknown, so Eq. (5) should be used. And  $\mathbf{u}_{mid}$  can be calculated by

$$\begin{cases} \mathbf{u}_{mid}^1 = (0.5\mathbf{u}_w + (0.5 - \delta)\mathbf{u}_{fb}) / (1.0 - \delta) \\ \mathbf{u}_{mid}^2 = (1.5\mathbf{u}_w - (\delta - 0.5)\mathbf{u}_{f2}) / (2.0 - \delta) \\ \mathbf{u}_{mid} = \lambda(1 - \delta)\mathbf{u}_{mid}^1 + (1.0 - \lambda + \lambda\delta)\mathbf{u}_{mid}^2 \end{cases} . \tag{6}$$

Where  $\mathbf{u}_w$  is the moving boundary velocity.  $\delta = |\mathbf{r}_w - \mathbf{r}_b| / |\mathbf{r}_{fb} - \mathbf{r}_b|$ .  $\lambda$  is the parameter that balance the accuracy and stability.

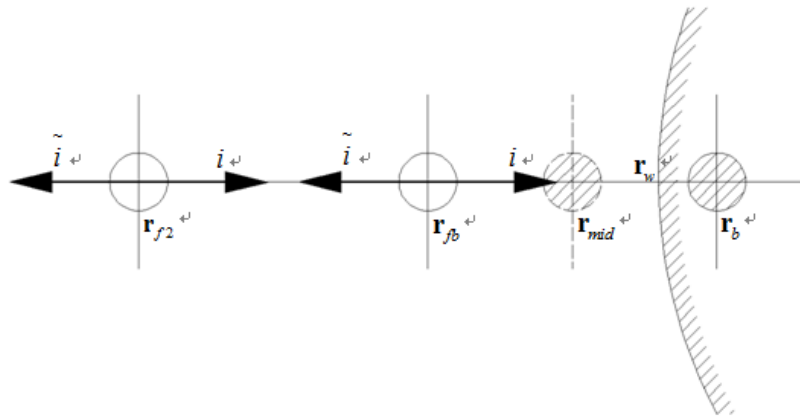


Figure 1 – Illustration of the fluid-structure boundary scheme

### 3. RESULTS AND DISCUSSION

In this section, this work carried out numerical simulation of viscous flows to flow past square and circular cylinders at  $Re=150$  with the help of calculation code in order to decrease the influence of inflow, outflow and wall boundary conditions. First, kept cylinder stationary and then explored the effect of flow law for the circular cylinder with a rotating speed. The computational domain of  $1600 \times 420$  was chosen and the distance between cylinder boundary and the channel wall surface is not less than 4 times characteristic dimensions. Two columns placed side-by-side, spaced 0.5 characteristic dimensions, the distance from the entrance of 380.

#### 3.1 Two Stable Columns in Cross Flow

Keeping the two columns stable, the flow dynamics around two side-by-side rigid columns and the forces on them in a cross flow at  $Re = 150$  is investigated. It was used a parabolic velocity profile at channel inlet, with maximum velocity of  $u_{max} = 0.1$  on the axis. Also, in order to verify the correctness of the model with flow-solid boundary, it was investigated flow characteristics flow past square and circular cylinders of  $1600 \times 360$  by varying the computation domain size at  $Re=150$ . The results are shown in table 1:

Table 1 – Comparison of the mean  $Cd$  and  $Str$  between literatures (20, 21) and present study

	Circular column		Square column	
	$Cd$	$Str$	$Cd$	$Str$
Literature (20)	1.2610	0.1790		
literature (21)			1.3210	0.1467
Isolated columns	1.2652	0.1766	1.3970	0.1470
Coupled columns	1.4159		1.7706	

Not only the results of isolated columns but those of coupled columns in a cross flow are shown in Table 1. By comparing the results like  $Cd$  and  $Str$  of isolated columns with literatures (20, 21), it can be found that the flow over column model is right. Also, the results show that  $Cd$  values of columns are both increased on the effect of interaction. More detail information will be discussed in the next.

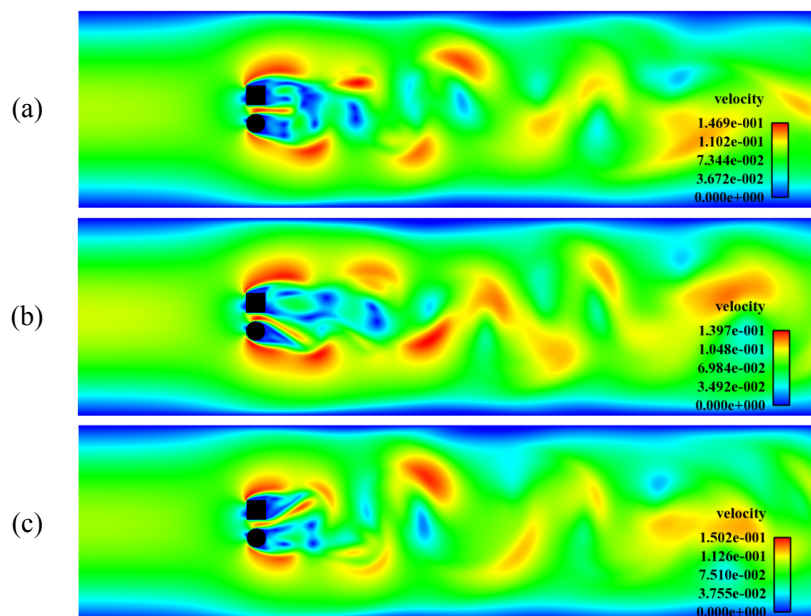


Figure 2 – Velocity pattern of two stable columns at three key time points.  
(a)  $t = 53000$ ; (b)  $t = 57000$ ; (c)  $t = 63000$

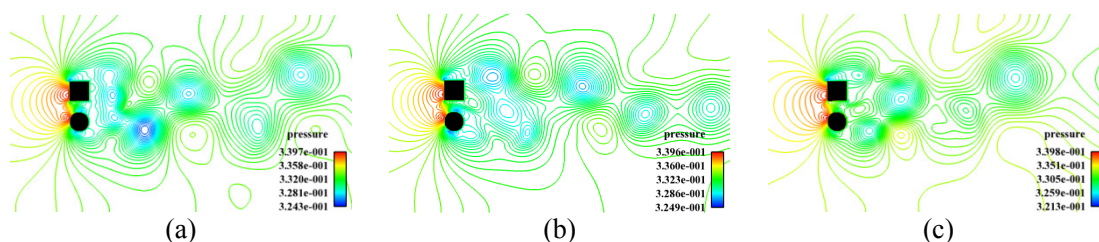


Figure 3 – The pressure pattern of the two side-by-side cylinders at  $Re = 150$   
(a)  $t = 53000$ ; (b)  $t = 57000$ ; (c)  $t = 63000$

Figure 2 shows the velocity pattern of two stable columns in a cross flow at  $Re = 150$ . Figure 3 shows the corresponding pressure counters around the two columns. By comparing the velocity pattern at three key time points in Figure 2, the irregularly periodic phenomena can be found what is different with the phenomena of isolated column. Three high velocity regions appear in Figure 2. They are separately the outsides of square and circular column, and the gap between the two columns. The high velocity region in the gap expresses the periodic fluctuation that divides the two vortices behind the two columns. In Figure 3, only one main high pressure region appears in front of the two columns. Due to the high velocity of the fluid, the high velocity regions in Figure 2 become low pressure regions in Figure 3. It can be observed that a periodic low pressure area formed in the downstream of the two columns, and the accumulation areas of complex multi-low pressure are produced close to the tail of columns. The boundary-layer separation points of two columns significantly changed. The boundary layer separation points do not change significantly on the side of the square cylinder away from circular cylinder. However the point does forward movement on

the side of circular cylinder away from square cylinder. Because of strong coupling interaction, it is obvious late that the separation happens on the sides of the two columns adjoining to each other and separation points are close to the end of column.

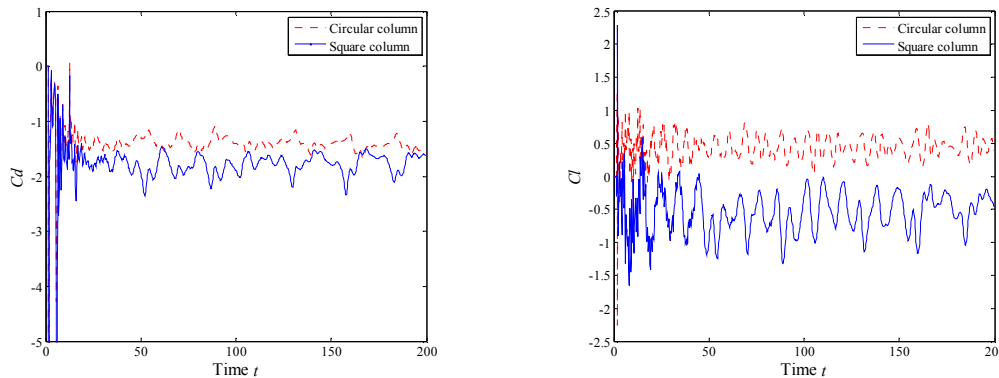


Figure 4 – The comparison of  $C_d$  and  $C_l$  of the two side-by-side columns at  $Re = 150$

The figure 4 shows the curves of drag and lift coefficients varying to time produced in the flow around two columns at  $Re=150$  and  $\delta_s / D = 0.5$ . From table 1 and figure 4(a),(b), it is obviously observed that the average drag coefficient of square cylinder is larger than that of circular cylinder. The absolute values of lift coefficient both are about 0.5, but the volatility of square cylinder is much greater. Compared with standard periodic volatility, Figure 4 shows the regular fluctuations become more disordered in the coupling interaction between two columns.

### 3.2 Effect of Rotating Velocity

The computational conditions is kept as  $1600 \times 420$ ,  $S / D = 0.5$ ,  $u_x = 0.1, u_y = 0.0$  and  $Re = 150$ . Then, the characteristics of flow over the two columns while the circular cylinder rotating at  $w = 0.0001, 0.0002, 0.0003$  are researched.

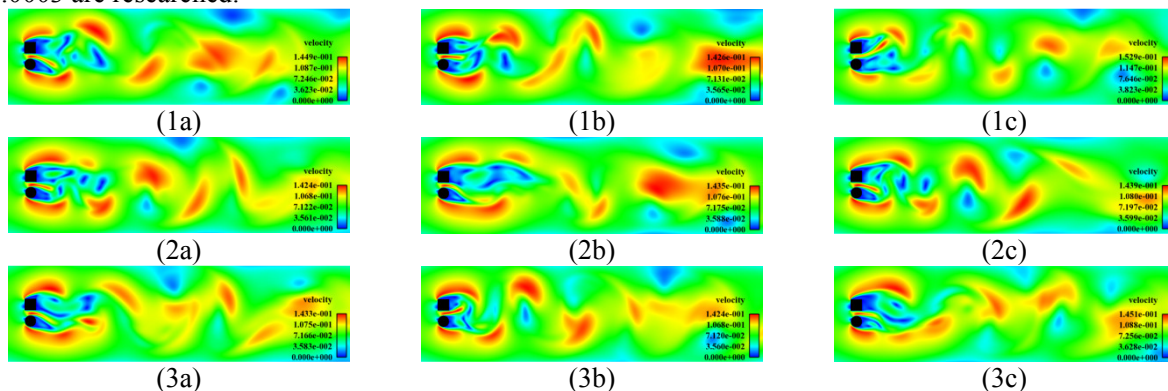
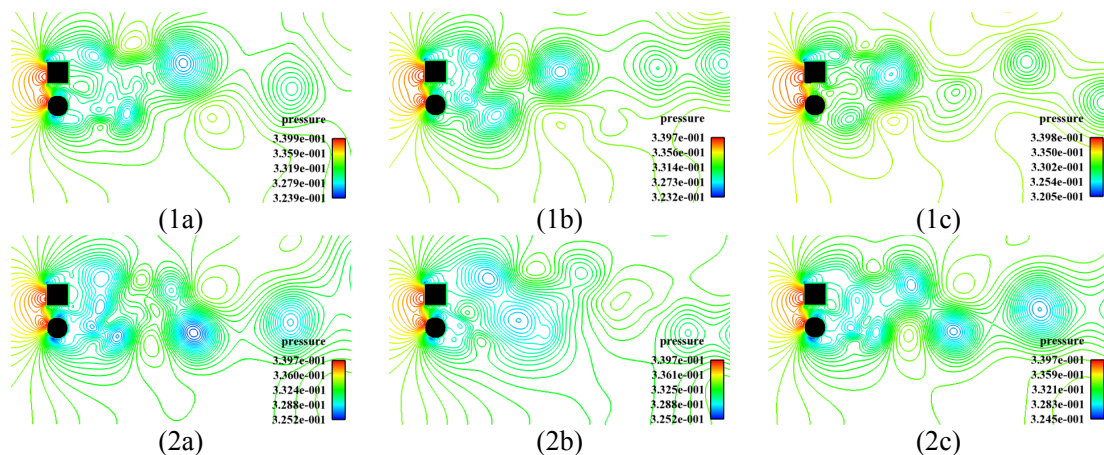


Figure 5 – The velocity pattern of the two side-by-side cylinders when the circular column with a const velocity. The numbers stand for the rotating velocity: (1)  $w = 0.0001$ ; (2)  $w = 0.0002$ ; (3)  $w = 0.0003$ . The letters stand for the time point: (a)  $t = 53000$ ; (b)  $t = 57000$ ; (c)  $t = 63000$ .



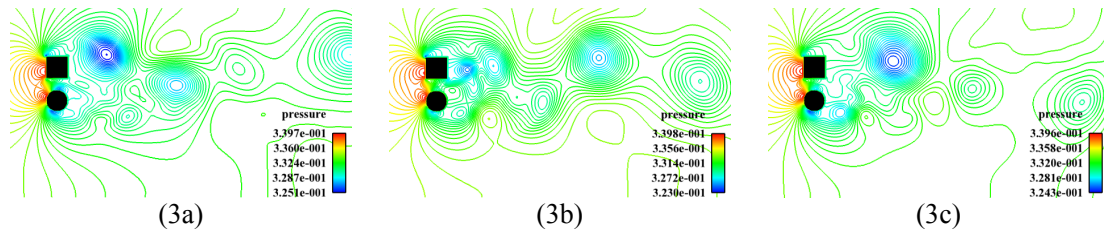


Figure 6 – The pressure contour of the two side-by-side cylinders when the circular column with a const velocity. The numbers stand for the rotating velocity: (1)  $w = 0.0001$ ; (2)  $w = 0.0002$ ; (3)  $w = 0.0003$ . The letters stand for the time point: (a)  $t = 53000$ ; (b)  $t = 57000$ ; (c)  $t = 63000$ .

Figure 5 shows the velocity distributions of two columns at three key time ( $t = 53000, 57000, 63000$ ) when the circular cylinder rotates separately at  $w = 0.0001, 0.0002, 0.0003$ . Figure 6 shows the corresponding pressure equipotential lines around columns. The results show that the variations of velocity and pressure distribution around columns are no obvious difference in the three cases. In the condition of  $\delta s / D = 0.5$ , there are not four rows of vortex structure parallel distributing downstream the columns that of  $\delta s / D > 2.0$ . The phenomenon of periodic pendulum occurs in high speed region between the two columns in figure 5. Furthermore, multiple vortexes formed close to the columns seem to be more complex, and as the flow goes they will merge into a large vortex, and then comes off.

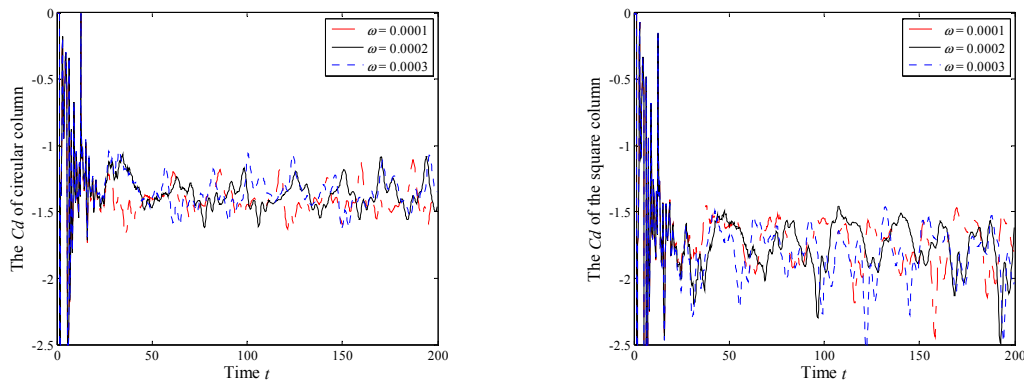


Figure 7 – The comparison of  $Cd$  of the circular and square cylinders with different rotating velocity

Figure 7(a) and (b) show the curves that the drag coefficients of the circular cylinder and the square cylinder with different rotating speed. The results show that the drag coefficients of the two columns are not influenced obviously by the rotating velocity which is not high. Under the three rotating speeds, the average drag coefficient of the circular cylinder is about 1.4, and that of the square cylinder is about 1.8. As the angular speed increases, the largest volatility amplitudes of the two columns are increased and the volatility amplitude of square cylinder is much larger than that of the circular cylinder. Besides, the drag coefficient of square cylinder produces asymmetric fluctuation.

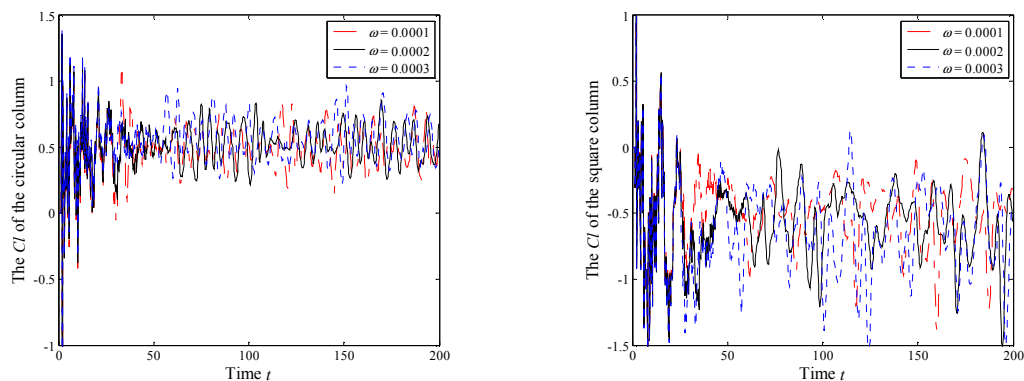


Figure 8 – The comparison of  $Cl$  of the circular and square cylinders with different rotating velocity

Figure 8(a) and (b) separately show the curves that the lift coefficients of the two columns with different rotating speed. The average lift coefficient of circular cylinder is about 0.5, and square cylinder is about 0.6. As the discovery about drag force, the circular cylinder rotation does not change the average lift coefficient of the two columns obviously. As the angular speed increases, the volatility amplitudes of lift coefficient are both increased and the volatility amplitude of the square cylinder is

larger than that of the circular cylinder.

#### 4. CONCLUSION

Based on the lattice Boltzmann method (LBM), the plane and curved wall were dealt by using the Half-way rebound boundary combining with the finite difference method, and a model of flow around bodies where one is a rotative circular cylinder and the other is a stationary square cylinder in viscous flow field is established. The characteristics of flow around two columns when the two columns were static and circular cylinder rotates at a certain speed are investigated at  $Re=150$ . It can be concluded that:

- 1) Relative to flow around a single cylinder, vortex shedding in the condition of two columns coupling with each other is more complex. And the average drag coefficients of the flow around circular and square cylinders both are increased obviously. Meanwhile, the absolute value of the lift coefficient of the two columns will not be zero.
- 2) Significant changes have taken place in the location of separate point of boundary layer on the circular and square cylinders under the coupling interaction. On the side of square cylinder departing from the circular cylinder, the separate point is still the angle point of the square cylinder. But on the side of the circular cylinder departing from the square cylinder, the separate point is advanced along the inflow direction. In the gap between the two columns, the separate point locations on the two columns are both left behind obviously.
- 3) Within the range of speeds studied in this work, the average drag coefficient and lift coefficient are not influenced clearly by this factor. But it is found that the rotating velocity can seriously cause the drag and lift coefficients vibration, and the larger the speed is, the larger the fluctuation is. The drag coefficient of the square cylinder will produce a specially strong vibration in one direction when circular cylinder rotates.

#### ACKNOWLEDGEMENTS

This paper is funded by the International Exchange Program of Harbin Engineering University for Innovation-oriented Talents Cultivation. And the authors are grateful to the Program of the Scientists Fund for Outstanding Young Scholars of China (Grant No. 51222904) and the Program for New Century Excellent Talents in University (Grant No. NCET100054) for support.

#### REFERENCES

1. Yong X, De-Tang L, Yang L. Lattice Boltzmann simulation of the cross flow over a cantilevered and longitudinally vibrating circular cylinder. *Chinese Phys Lett*. 2009; 26(3): 034702.
2. Murakami S, Mochida A. On turbulent vortex shedding flow past 2D square cylinder predicted by CFD. *J Wind Eng Ind Aerod*. 1995; 54: 191-211.
3. Saha A K, Biswas G, Muralidhar K. Three-dimensional study of flow past a square cylinder at low Reynolds numbers. *Int J Heat Fluid Fl*. 2003; 24(1): 54-66.
4. Kim Y, Peskin CS. 3-D Parachute simulation by the immersed boundary method. *Comput Fluids*. 2009; 38(6): 1080-1090.
5. Zhou H, Mo G, Wu F. GPU implementation of lattice Boltzmann method for flows with curved boundaries. *Comput Meth Appl M*. 2012; 225: 65-73.
6. Yu D, Mei R, Luo LS. Viscous flow computations with the method of lattice Boltzmann equation. *Prog Aerosp Sci*. 2003; 39(5): 329-367.
7. Qian YH, d'Humières D, Lallemand P. Lattice BGK models for Navier-Stokes equation. *EPL (Europhysics Lett)*. 1992; 17(6): 479.
8. He X, Doolen GD. Lattice Boltzmann method on a curvilinear coordinate system: Vortex shedding behind a circular cylinder. *Phys Rev E*. 1997; 56(1): 434.
9. Ziegler DP. Boundary conditions for lattice Boltzmann simulations. *J Stat Phys*. 1993; 71(5-6): 1171-1177.
10. Niu XD, Shu C, Chew YT. A momentum exchange-based immersed boundary-lattice Boltzmann method for simulating incompressible viscous flows. *Phys Lett A*. 2006; 354(3): 173-182.
11. Noble DR, Chen S, Georgiadis JG. A consistent hydrodynamic boundary condition for the lattice Boltzmann method. *Phys Fluids*. 1995; 7(1): 203-209.
12. Lallemand P, Luo LS. Lattice Boltzmann method for moving boundaries. *J Comput Phys*. 2003; 184(2): 406-421.
13. Shu C, Jie W. A new immersed boundary-lattice boltzmann method and application to incompressible

- flows. *Mod Phys Lett B*. 2009; 23(3): 261- 264.
14. Shi DY, Wang ZK, Zhang AM. A novel lattice Boltzmann method dealing with arbitrarily complex fluid-solid boundaries. *Acta Phys Sin*. 2014; 63(7): 074703.
  15. Agrawal A, Djenidi L, Antonia RA. Investigation of flow around a pair of side-by-side square cylinders using the lattice Boltzmann method. *Comput Fluids*. 2006; 35(10): 1093-1107.
  16. Xu Y, Liu Y, Xia Y. Lattice-Boltzmann simulation of two-dimensional flow over two vibrating side-by-side circular cylinders. *Phys Rev E*. 2008; 78(4): 046314.
  17. Hong-Bing Y, Yang L, You-Sheng X. Numerical Simulation of Two-Dimensional Flow over Three Cylinders by Lattice Boltzmann Method. *Commun Theor Phys*. 2010; 54(5): 886.
  18. Patil DV, Lakshmisha KN. Two - dimensional flow past circular cylinders using finite volume lattice Boltzmann formulation. *Int J Numer Meth Fl*. 2012; 69(6): 1149-1164.
  19. Xu K, He X. Lattice Boltzmann method and gas-kinetic BGK scheme in the low-Mach number viscous flow simulations. *J Comput Phys*. 2003; 190(1): 100-117.
  20. He X, Doolen G. Lattice Boltzmann method on curvilinear coordinates system: flow around a circular cylinder. *J Comput Phys*. 1997; 134(2): 306-315.
  21. Breuer M, Bernsdorf J, Zeiser T. Accurate computations of the laminar flow past a square cylinder based on two different methods: lattice-Boltzmann and finite-volume. *Int J Heat Fluid Fl*. 2000; 21(2): 186-196.